

Thermal Control Technologies for Europa Clipper Mission

Pradeep Bhandari¹, A. J. Mastropietro², Razmig Kandilian³, Jenny Hua⁴, Sean Reilly⁵, Paul Woodmansee⁶, Tyler Schmidt⁷, Mark Duran⁸

Jet Propulsion Laboratory, California Institute of Technology, Pasadena, CA 91109

The Europa Clipper Mission to Europa, a moon of Jupiter, is planned for a launch in 2023. Since Europa is at a large distance (5.6 A.U.) from the Sun, the solar flux is less than 4% of that at Earth. This requires very large solar arrays to meet the power demands of a typical new mission concept. Hence, conservation of power for use in thermal control is extremely important. To achieve this goal a mechanically pumped fluid loop heat rejection system (HRS) is utilized to harvest waste heat from the spacecraft components. In addition to this, several thermal control technologies are employed. They include a high performance dual Multi-Layer Insulation (MLI) blanket design to minimize the large majority of heat loss from the spacecraft; two passive thermal control valves in series to greatly reduce the heat loss from the HRS to its radiator; and a low temperature louver to further reduce the loss from the radiator. This paper will describe these technologies, schemes for their implementation, and results of development tests to validate their performance.

Nomenclature

<i>HRS</i>	=	heat rejection system
<i>UC</i>	=	upper cylinder
<i>LC</i>	=	lower cylinder
<i>PM</i>	=	propulsion module
<i>PRT</i>	=	platinum resistance thermometer
<i>RF</i>	=	radio frequency
<i>REM</i>	=	rocket engine module
<i>RW</i>	=	reaction wheel
<i>RHB</i>	=	replacement heater block
<i>RCS</i>	=	reaction control system
<i>WCC</i>	=	worst case cold
MLI	=	Multi-Layer Insulation
CTE	=	Coefficient of Thermal Expansion

¹ Principal Thermal Engineer, Propulsion, Thermal, and Materials Systems, 4800 Oak Grove Drive, Pasadena, CA 91109, M/S 125-123

² Senior Thermal Engineer, Spacecraft Thermal Engineering, 4800 Oak Grove Drive, Pasadena, CA 91109, M/S 125-123

³ Thermal Engineer, Spacecraft Thermal Engineering, 4800 Oak Grove Drive, Pasadena, CA 91109, M/S 125-123

⁴ Thermal Engineer, Instrument and Payload Thermal Engineering, 4800 Oak Grove Drive, Pasadena, CA 91109, M/S 125-123

⁵ Thermal Engineer, Spacecraft Thermal Engineering, 4800 Oak Grove Drive, Pasadena, CA 91109, M/S 125-123

⁶ Senior Propulsion Engineer, Chemical Propulsion and Fluid Flight Systems, 4800 Oak Grove Drive, Pasadena, CA 91109, M/S 125-123

⁷ Thermal Engineer, Spacecraft Thermal Engineering, 4800 Oak Grove Drive, Pasadena, CA 91109, M/S 125-123

⁸ Thermal Engineer, Analytical Chemistry and Materials Development, 4800 Oak Grove Drive, Pasadena, CA 91109, M/S 18-105

I. Introduction

The Europa Clipper Mission scheduled to launch in 2023 is a deep space planetary exploration mission with an objective to evaluate the potential habitability of Jupiter's icy moon Europa. Specifically, it aims to 1) characterize the icy shell of Europa and the properties of the subsurface water including ocean salinity and ice sheet thickness, 2) determine the chemical composition of the surface matter and the atmosphere including potential plumes, and 3) characterize the geology of the moon to aid with the selection of future landing sites as well as to understand the formation of magmatic, tectonic, and impact landforms. Figure 1 illustrates the Europa Clipper spacecraft showing the Vault, Radio Frequency (RF), and Propulsion Modules (PM) as well as thermal control components such as the replacement heater block (RHB) and the radiator.

It is a solar powered mission, and due to the large distance from the Sun (5.6 A.U.), the solar flux is only 4% of that on Earth. This requires very large solar arrays to meet the power demands of a typical new mission concept. Hence, conservation of power for use in thermal control is extremely important. To achieve this goal a mechanically pumped fluid loop heat rejection system (HRS) is utilized to harvest waste heat from the spacecraft components. HRS based thermal controlled systems, pioneered by JPL, have a long and successful flight history for the last 2 decades, starting from Mars Pathfinder, through the twin Mars Exploration Rovers, to Mars Science Laboratory Curiosity Rover Mission¹⁻²³. So this is now a well-established technology.

However, because of the severe scarcity of power in the Clipper Mission, additional thermal control technologies are employed. They include a high performance dual Multi-Layer Insulation (MLI) blanket design to minimize the large majority of heat loss from the spacecraft; two passive thermal control valves in series to greatly reduce the heat loss from the HRS to its radiator; a low temperature louver to further reduce the loss from the radiator. Some of these are extensions of existing technologies, while others are new.

To our knowledge, dual MLI blankets have not been flown before, particularly for this scale of a space system. Single blankets are used universally in all space flight missions. However, a dual blanket scheme was conceived of for this mission to provide significant reduction in the heat loss through them. Detailed analysis of this concept was conducted and a development test was performed to validate its performance.

Passive thermal control valves have been flown on all JPL HRS, but not in a configuration where two of them have been put in series to dramatically reduce flow rates in one of the two directions when that flow would be undesirable from the point of losing precious heat from the spacecraft to the radiator for the HRS. Extensive analysis and testing has been conducted to qualify this series combination for Clipper.

Louvers have a long history of spaceflight for several decades, but their operating temperatures have been in a relatively benign range (-50 C to +50 C). The current state of the art louver designs are not qualified for the temperature ranges the Clipper HRS radiator is predicted to be at during the worst case cold phase when the flow into the radiator is completely bypassed. In those conditions the radiator could reach temperatures as low as -100 C. A new louver bimetal spring was created for use in the existing louver and is being qualified for Clipper.

II. Key Characteristics of Europa Clipper Spacecraft

Figure 1 shows several views of the Europa Spacecraft in its current state & shows a schematic of the Europa Clipper HRS loop (Figure 2) servicing the following modules and components:

- a) Avionics Vault module where the electronic components reside
- b) Radio Frequency (RF) Module
- c) Replacement heater block (RHB), used to supply supplemental heat to the loop
- d) Rocket engine modules (REMs) each housing six reaction control system (RCS) thrusters
- e) Upper cylinder (UC) and lower cylinder (LC) of propulsion module
- f) Thermal control radiator used to reject excess heat

The REMs, RW, UC, and LC can be grouped together into the propulsion module (PM). The thermal control valve (TCV) functions to control the vault inlet temperature by modulating the flow rate to the radiator²⁴. The details of the TCV operation were described by Birur et.al. but are outside of the scope of this study. The valve was assumed to be fully open, i.e., 99.86% flow to radiator in the hot case, and fully closed, i.e., 0.16% flow to the radiator in the cold case. The flow rate of the pump used for the Clipper HRS is 1.5 lpm for a developed pressure difference of 152 kPa (22 psid) for the working fluid (CFC-11). The PM flow is split to minimize the pressure drop across it.

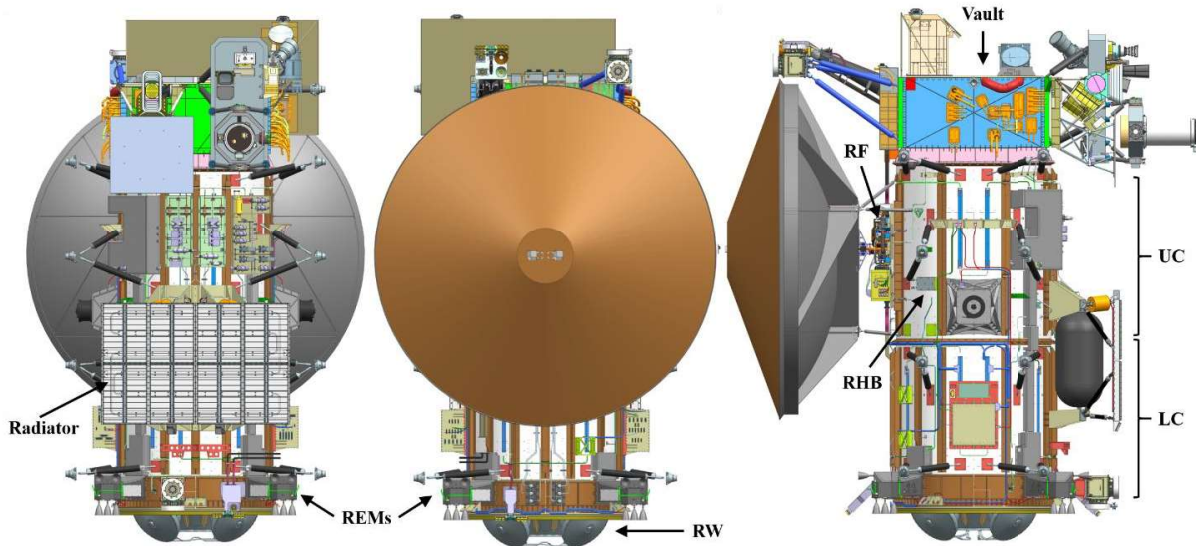
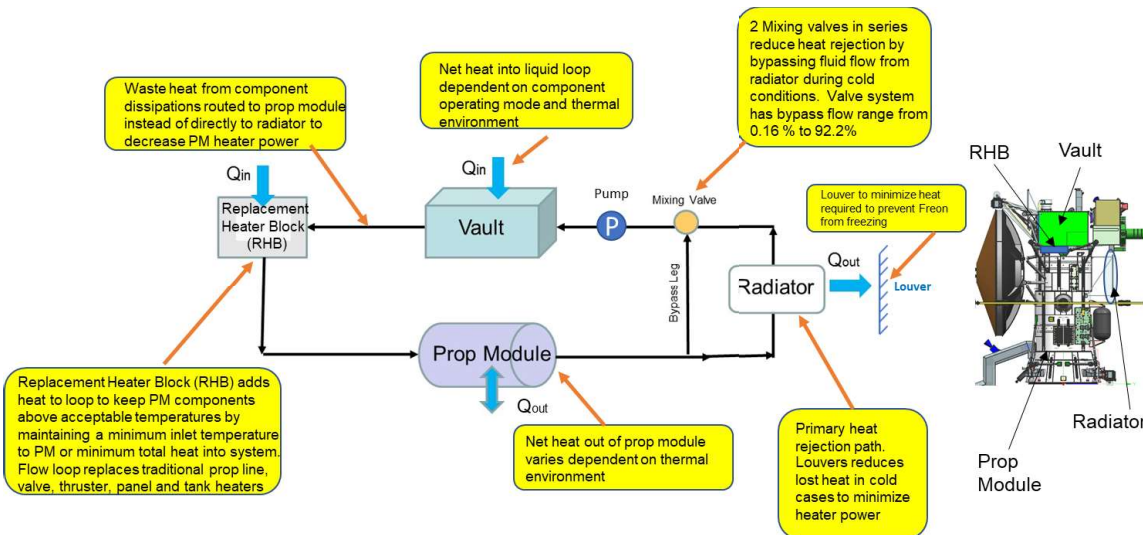


Figure 1. Europa Clipper spacecraft model showing the major modules and thermal control components.



HRS is designed to use component dissipations to warm up propulsion module

Figure 2. HRS flow diagram showing various components in the fluid loop.

III. Dual MLI Blanket

The primary motivation for this research was to develop MLI blanket concepts that could dramatically reduce the heat loss through these blankets. Another important consideration is to ensure that they are applicable to and implementable on typical spacecraft with complicated shapes, feedthroughs and penetrations. These concepts should also be robust for launch vibrations and loading. Several concepts that have been documented before in literature²⁴⁻²⁷ do provide significant improvements in MLI performance but they tend to be applicable to very simple shapes (simple rectangular, cylindrical in nature), are not very robust for launch loading, and are quite difficult to implement on complex shaped spacecraft. A detailed treatise on this concept has been documented in literature²⁸. This research was focused on expanding current MLI concepts that have been proven for implementation and are robust for launch and applicable to complicated shapes. Furthermore, these concepts have the same areal mass density as traditional MLI to ensure that they do not increase the blanket mass significantly.

For any MLI blanket, there are several key parameters that affect its effective emittance (ϵ^*): number of layers, layer density (how tightly/closely the layers are packed), seams (stitched edges) and MLI source/sink temperatures. In general increasing the number of layers decreases the ϵ^* , however beyond 20 layers or so, the relative improvement yields marginal returns at the expense of increased mass, which is usually not desirable. Detailed analysis and testing has shown the diminishing returns that would be realized by increasing the number of layers beyond ~20 because the ϵ^* vs. number of layers plot flattens out in an asymptotic fashion.

The layer density is extremely important because the more tightly packed the layers are, the more the layers touch each other and contact conduction between them starts to dominate the radiative isolation between adjacent shields. Keeping the MLI layers loose is most desirable but it is hard to achieve in real practice, particularly around corners when the layers inevitably get crushed (unless each layer is increasing slightly in area, but this requires significant labor to achieve this). Stitched seams are the ultimate form of increasing layer density because when the layers are crushed during the stitching process, they lead to a local increase in layer density, hence this is one of the biggest culprit in increasing ϵ^* .

The Lockheed equation is an empirical correlation derived from test data of various blanket designs at the Lockheed Corporation (now Lockheed Martin)²⁹. The equation accounts for the effects of layer density, the number of layers, seams, and temperature. The equation includes terms for conductive and radiative heat transfer through a blanket. The Lockheed equation is:

$$\epsilon^* = \frac{7.30 \cdot 10^{-8} N^{2.63}}{\sigma(N_s + 1)} \left(\frac{1}{T_h^2 + T_c^2} \right) + \frac{7.07 \cdot 10^{-10} (0.043)^{(2)}}{\sigma N_s} \left(\frac{T_h^{4.67} - T_c^{4.67}}{T_h^4 - T_c^4} \right) \quad (1)$$

Where N is the layer density (layers/cm), N_s is the number of layers, T_h is the hot sink temperature (K), T_c is the cold sink temperature (K), and σ is the Stefan-Boltzmann constant (W/m^2K^4). For a single blanket configuration, the blanket ϵ^* can be calculated by simply using the equation.

For a given set of source and sink temperatures, and with limitations of numbers of layers (to minimize mass), the dominant parameter is the layer density and the relative spacing of seams. Larger blankets have a smaller areal fraction of seams. Hence, they tend to be lower in ϵ^* . When the seams or layer density cannot be reduced, the only reasonable way to reduce the ϵ^* is to create separate blankets (nominally two blankets with same total number of layers as a single individual blanket to maintain the same mass). Then if the two separated blankets have low emissivity external layers facing each other (outer surface of first blanket and inner surface of second one), and since these layers have very low emissivities that are comparable to the ϵ^* of a MLI blanket, the additional thermal isolation between these two facing layers is in series with the ϵ^* of each of the two blankets. This provides significantly lower overall ϵ^* for the two blanket system when compared to that of a single full blanket. The main reason this provides that advantage when compared to the facing layers sewn together (as they would in a single full blanket) is that the conduction coupling between these two facing layers is eliminated. Figure 3 illustrates this concept.

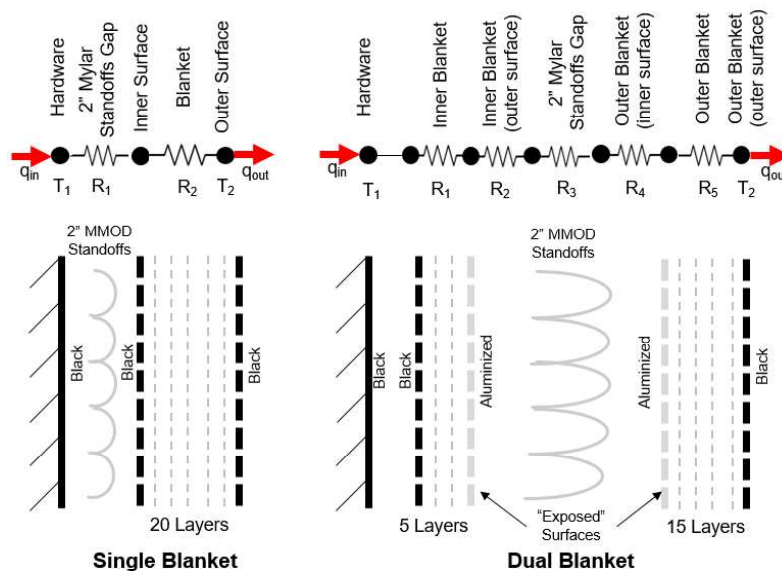


Figure 3. Single vs Dual Blanket Concept

Of course, two conditions have to be satisfied to achieve the potential improvement of this concept: the two blankets have to be kept separated by low or negligible thermal conductance standoffs (e.g., very thin standoffs of aluminized Mylar) and they need to have very low emissivities. Aluminized Mylar has an emissivity of approximately 0.04. A highly simplified example of a dual blanket vs. a single blanket is as follows: assume the first blanket has 5 layers and a ε^* of 0.05, the second blanket has a ε^* of 0.03 for 15 layers, the two inner exposed layers of the two blankets facing each other (and physically separated) have low emissivity surfaces of 0.04. For two equal area planar surfaces facing each other, the following simple radiation heat transfer equation provides the effective emittance, ε_{eff} , of the combination:

$$\frac{1-\varepsilon_1^*}{\varepsilon_1^*} + \frac{1}{\varepsilon_{1,o}} + \frac{1}{\varepsilon_{2,i}} + \frac{1-\varepsilon_2^*}{\varepsilon_2^*} = \frac{1}{\varepsilon_{eff}} \quad (2)$$

Where ε_1^* and ε_2^* are the effective emittances of the first and second blankets, respectively; and $\varepsilon_{1,o}$ and $\varepsilon_{2,i}$ are the emissivities of the exposed surfaces of the two blankets facing each other. Then using equation 1, the entire dual blanket system will have an overall ε_{eff} of $\left[\frac{1-0.05}{0.05} + \frac{1}{0.04} + \frac{1}{0.04} + \frac{1-0.03}{0.03} \right]^{-1}$ or 0.01. For the single blanket with 20 layers the ε^* would be $\left[\frac{1-0.05}{0.05} + \frac{1-0.03}{0.03} \right]^{-1}$ or 0.02. This simple example illustrates how to reduce overall ε^* by half compared to single blankets by separating the two sub-blankets with low emissivity facing inner layers.

To investigate the potential for reducing MLI ε^* by using a separated dual blanket scheme, a series of development tests were conducted in January & February of 2018. Prior to testing, predictions were made for the expected performance during the test and then compared to those measured. This development test was designed to characterize the performance of various MLI blanket constructions and configurations. MLI performance is particularly important for deep space solar array powered missions where power conservation drives the design at high AU distances. Therefore, blanket design improvements learned from this test would be beneficial to Europa Clipper, and other potential future missions. The key objectives of this test were to characterize overall effective emissivity, ε^* , of several MLI blanket configurations, particularly those involving dual blanket configurations.

The list of all tested blanket constructions and configurations is in Table 1. Each blanket had five sides with sewn seam edges and a sixth side that acted as a flap, which was closed out just before testing. Each of the blankets was tested at test article temperatures of roughly +20, +35, and +50 °C. This provided several data points to characterize the change (if any) in blanket performance over a temperature range within limits for many components on the Europa Clipper spacecraft. It was determined by analysis that the conduction coupling via the spacers was insignificant due to the cross section of heat flow through them being very small and the MLI layers being very poor conductors in their lateral surface direction (limiting thermal shorting to very small fraction of areas of these layers). The penetrations & wire harnesses will be simulated in the development tests to assess their impact on heat loss.

The primary objective of this development test was to determine if any of the dual blanket concepts could reduce the heat loss from that of the 20-layer single blanket baseline. Table 1 shows the condensed version of the predicted and test actual ε^* values for all test cases using the larger blanket areas. All of the dual blanket concepts (except case 3 which had carbon filled black Kapton surfaces) had a roughly two times reduction in ε^* from the baseline blanket design. Since ε^* is a direct measure of the heat loss per unit area, it shows that a dual blanket has the potential to reduce the heat loss by factor of two. Additionally, the use of Dacron netting vs. embossed aluminized kapton or normal vs. staggered seams made little impact on the blanket performance. The test cases that used two 15 layer blankets did not show improvement over a 5 and 15 layer blanket configuration.

This development test has shown that dual blanket concepts are viable for reducing heat loss per unit area by factor of two from that of a single blanket on a small-scale. Most dual blanket cases resulted in roughly half the heat loss of a standard 20-layer blanket. Changes in the blanket layout (Dacron vs. embossed) and seams (normal arrangement vs. staggered) had little impact on the results in this test. A full-scale test using thermal pathfinder models of the actual flight hardware is planned to validate the blanket's performance. That test should validate the findings of this test and determine more realistic values for blanket performance in a more flight-like configuration that includes feedthroughs and realistic geometry.

Case	Blanket Scheme	Total Predicted ϵ^*	Total Test ϵ^*	Test/Predict	Case #/ Case 1 (Test)
1	20 CK, DAM, CK	0.0177	0.0150	0.85	-
2	20 CK, DAM, CK (extra seams)	0.0202	0.0354	1.75	2.36
3	5 CK, EAK, CK + 2" + 15 CK, DAM, CK	0.0137	0.0128	0.93	0.85
4	5 CK, EAK, AM + 2" + 15 AM, DAM, CK	0.0070	0.0068	0.97	0.45
5	5 CK, DAM, AM + 2" + 15 AM, DAM, CK	0.0070	0.0075	1.07	0.50
6	5 CK, EAK, AM + 2" + 15 AM, DAM, CK (staggered seams)	0.0067	0.0072	1.07	0.48
7	2" + 5 CK, EAK, CK + 15 CK, DAM, CK (staggered seams)	0.0091	0.0080	0.88	0.53
8	15 CK, EAK, AM + 2" + 15 AM, DAM, CK	0.0051	0.0079	1.55	0.53
9	15 CK, EAK, AM + 2" + 15 AM, DAM, CK (staggered seams)	0.0049	0.0086	1.76	0.57

**Table 1. Comparison between predicted and test values (using larger of two blanket areas where applicable).
Blanket Layup Sequence: CK = carbon filled black kapton; AM = aluminized Mylar; EAK = embossed aluminized Kapton; DAM = Dacron netting and aluminum Mylar**

This concept has been baselined (Figure 4) in Europa Clipper for application of this dual MLI concept. The first is the Europa Clipper mission that is slated to launch as early as 2023. The Europa Clipper spacecraft features a large propulsion module with a cylinder that is maintained between 0 and +35 °C. The cylinder is where an MLI concept from this development test could be best implemented.

The proposed implementation for a dual blanket scheme on Europa Clipper is illustrated in Figure 4. The outer blanket would be supported by structural ribs that appear circumferentially around the prop module cylinder. Pairs of 2.5 mm holes cut into the ribs would be used as lacing cord tie down features for supporting the blanket. The inner blanket would be sized for a conformal fit of the cylinder and fill the gaps between the structural ribs. Aluminized Mylar standoffs would be placed in the gap between the blankets to maintain an offset and provide additional structure support to the outer blanket.

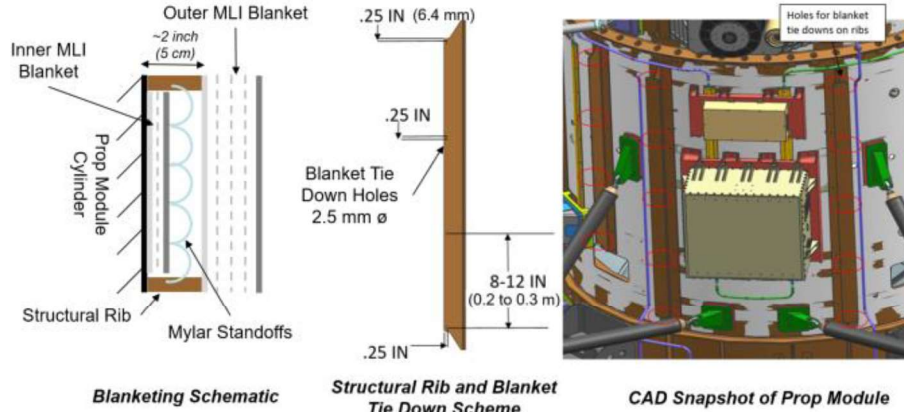


Figure 4. Proposed implementation of dual blanket scheme on Europa Clipper propulsion module

IV. Two Passive Thermal Control Valves in Series

As shown in Figure 5, a passive thermal control valve is employed to bypass the HRS radiator in cold conditions to conserve heat. This valve automatically recirculates the flow into the HRS tubing attached to the components controlled by the HRS during the cold conditions. Conversely, during hot conditions, the same valve automatically directs the fluid to the radiator when excess heat needs to be rejected to maintain the HRS controlled components' temperatures within their allowable limits. A pair of these thermal control valves and the pumps is employed to create a single fault tolerant system to overcome a failure of either unit.

This thermal control valve is totally passive and is actuated by the thermal expansion (or contraction) of an oil (DC-200) that has a very high Coefficient of Thermal Expansion (CTE)³⁰. When the fluid flows coming into this valve from the radiator (cold) & the exit of the propulsion module (hot), the resultant mixed temperature of the fluid expands or contracts the DC-200 contained in a welded bellows. This leads to a linear motion of the spool connected to this bellows, which in turn opens or closes ports oriented to these two inflows of HRS fluid. So based on the set points of this valve (relative positioning of the two ports with respect to the moving spool), the mixed fluid exiting this valve (towards the pump) is controlled within the dead-band of the set points.

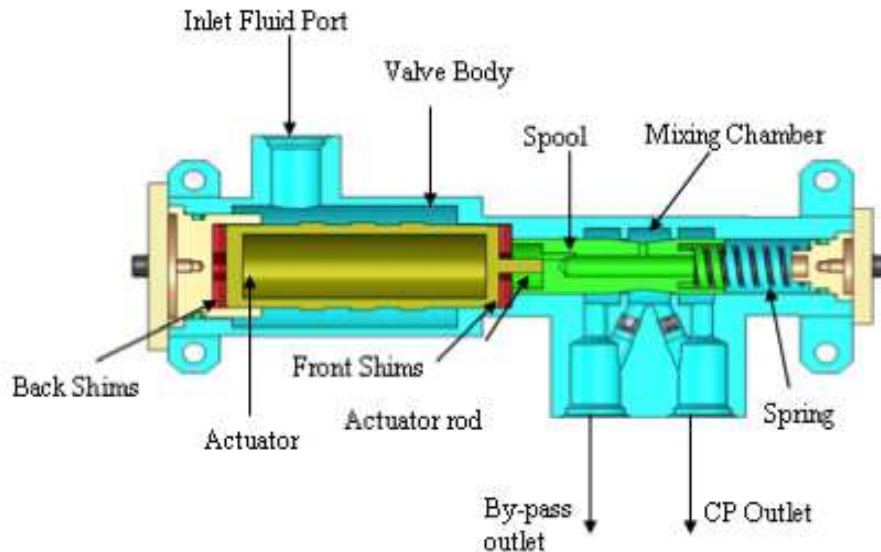


Figure 5. Passive Thermal Control Valve

The two ports openings flow areas primarily control the flow split within the valves incoming fluids. The spool within the valve housing has a very close fit to avoid any flow leakage in the axial direction, which would lead to some parasitic flow into the radiator during cold conditions. Ideally, one would desire this leak flow to be zero to

minimize heat loss from the HRS to the radiator. However, due to the concern with the valve spool jamming within the valve's housing when the radial gap is made extremely small, a small radial gap is allowed for to mitigate this concern. This leads to an inevitable leak flow that would result in an undesirable heat loss to the radiator. This is a risk vs. performance trade. Robustness of this design over a duration greater than a decade in flight is extremely important, hence the need for a small radial clearance.

Unfortunately, there is still a very large power price to pay for buying this robustness. In order to overcome this penalty, a scheme was conceived that places two such thermal control valves in series, as shown schematically in Figure 6. The mixed exit flow of the upstream valve enters one port of the downstream valve (V_1), while the second port of the downstream valve allows the flow exiting from the propulsion module.

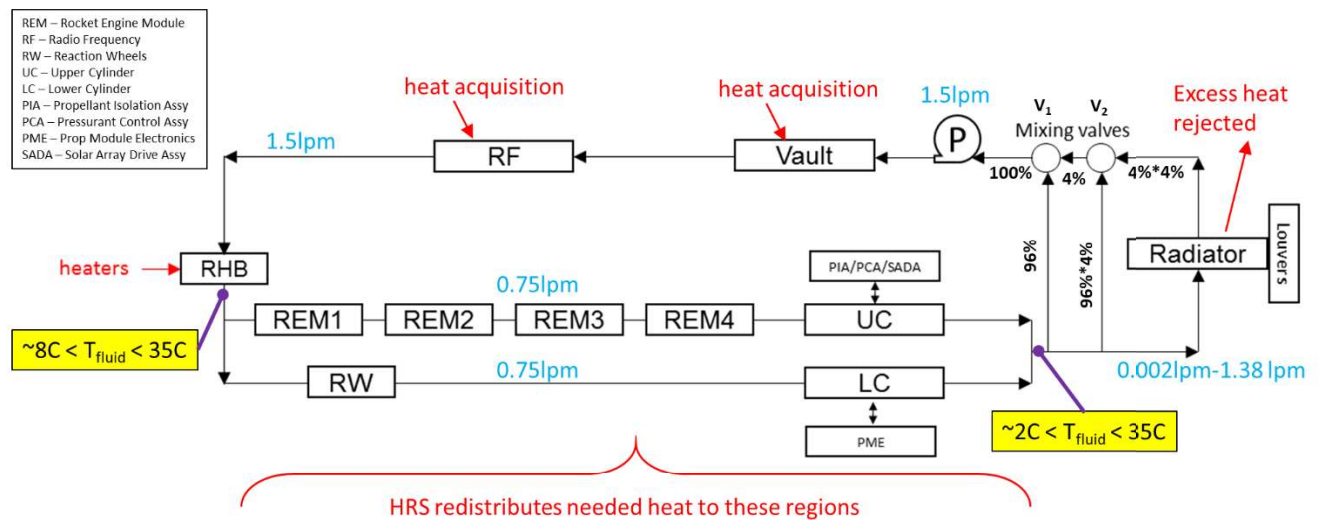


Figure 6. HRS flow diagram showing various components in the fluid loop & Dual Passive Thermal Control Valves

During cold conditions, the cold flow entering these valves from the cold radiator closes their ports in the radiator direction but opens the ports in the radiator bypass direction. As a result, the radiator flow is throttled down due to their set points. However, as discussed before, there is a limit to how much one can close the flow in the radiator's direction to avoid jamming of these valves. In this combination of the two valves in series, the upstream valve (V_1) further throttles the flow going into the radiator because the flow impedances of the two valves are in series (the two bypass flows have very low impedances because they are wide open in that direction).

A numerical example in Figure 6 illustrates the above observation as follows: per the current design of these valves the lowest leak rate of each of them is about 4%. The downstream valve (V_1) would flow 96% of the total (100%) system flow in the bypass direction, and 4% entering it in the other direction. This 4% flow entering V_1 is also the flow leaving V_2 as its mixed flow. Hence the flow entering V_2 from the radiator is then 4%*4% of the total system flow or 0.16% of total system flow. Therefore, the two valves in series restrict the radiator flow to a mere 0.16% of the total system flow. This is in spite of each valve having a non-bypass flow of 4% of the total mixed flow in each individual valve. By this simple concept the flow in the radiator during cold conditions is restricted to a trickle flow, much lower than what would be the case for a single valve.

The importance of this flow in the radiator being very small is illustrated by the following numerical example: The total system flow is 1.5 lpm of CFC-11 which translates to a flow heat capacity (mdot*Cp) of 30 W/C. The flow leaving the propulsion module is at ~2 C in the cold conditions, and due to the radiator being at ~ -95 C in those conditions of trickle flow through it, the fluid experiences a temperature change of 97 C. If only a single valve were to be employed, the flow through the radiator would be 4% or a flow heat capacity of 4%*30 or 1.2 W/C. The resultant heat loss to the radiator via this 4% flow and a 97 C temperature drop would be extremely large, on the order of 100 W. As a matter of perspective, the total heat loss from the spacecraft is on the order of 300 W, so this would be an enormous penalty indeed. The actual value will not be as high because for this large heat input, the radiator would be correspondingly much warmer, leading to smaller temperature drop of the HRS fluid. The actual value would be about 40 W because the radiator would be at -30 C due to this heat from the HRS flow. But this simple calculation

gives a feeling for the penalty associated with a single valve. Comparing this to a two valves in series case, the corresponding heat loss would be only $0.16\% \cdot 30 \cdot 97$ or only 5 W, which is a huge reduction in wasted heat (an order of magnitude smaller).

During hot conditions, this configuration does not affect the performance of the HRS because with both valves open in the radiator direction (bypass direction closed for both), the flow impedance of these valves for the radiator flow is very small, hence the two impedances in series (open valves in radiator direction) do not change the flow in the radiator by any significant means.

A development test was conducted to validate this concept and it confirmed that the two valves in series reduce the flow in the radiator during cold conditions to a value even smaller than predicted as a product of the two individual valve leak rates. One key assumption is that two valves are at the same temperature. The valves' temperatures are influenced by the flowing fluid's thermal coupling to the valve housing and its thermal coupling to the pump assembly within which the valve is housed. If the housing is at a significantly different temperature than the valve, it could make its temperature (as well as the fluid flowing through it) different from the intended mixed fluid temperature because of any parasitic heat into it. To minimize this effect, the valves are thermally isolated from the pump assembly housing.

V. Low Temperature Louver

Traditional louvers rely on a relatively narrow allowable temperature range of -50 C to $+50\text{ C}$, with an operational (control range or dead-band) of about 20 C within this³¹. In the case of Clipper (Figure 7), since the heat flow to it from the HRS flow is designed to be minimal ($<10\text{ W}$), the radiator attains a very low temperature of $\sim -95\text{ C}$. This is below the low allowable limit of -50 C for traditional louvers. Hence a study was conducted with Sierra Nevada Corporation (SNC), who supplies these louvers for the Clipper radiator, to develop a louver design that is capable of surviving -95 C . Additionally, it should be in a completely closed position at temperatures below -95 C to minimize heat loss from the radiator (the louver's effective emissivity would be 0.14 when fully closed). Finally, it should also be completely open at temperatures $> 0\text{ C}$ to ensure that the radiator would be able to lose all the heat coming into it from the HRS flow, with the louver being fully open (the louver's emissivity is 0.74 when fully closed) during hot conditions. During hot conditions, with the louver fully open, the radiator could be as hot as 50 C (including a 20 C margin). This requires its survival range to be $\sim 150\text{ C}$, which is significantly larger than the 100 C for traditional louvers.

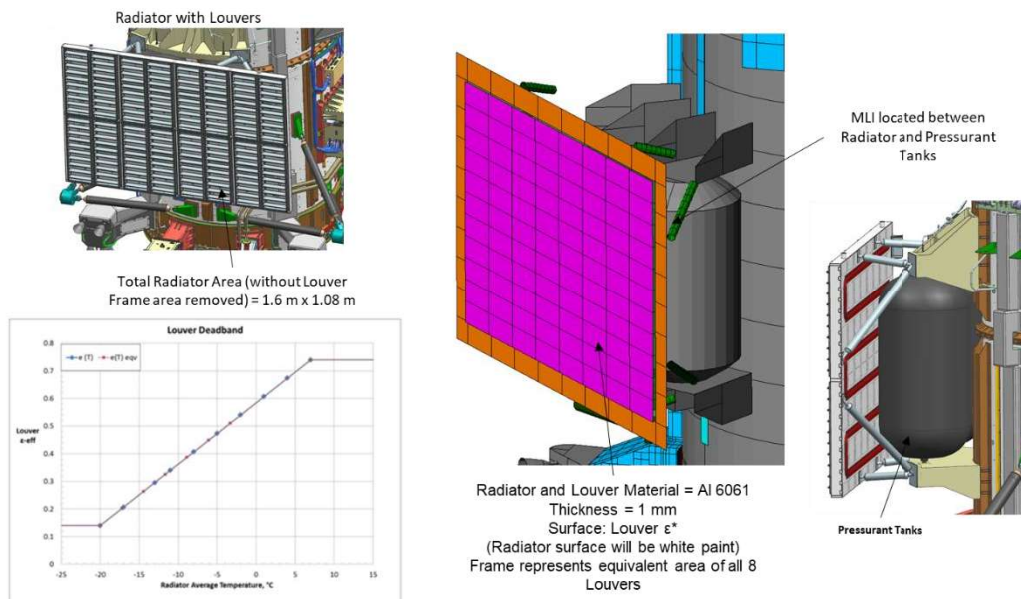


Figure 7. Louver on Clipper Radiator

One alleviating factor in the control range is that it can be allowed to be much larger than 20 C for traditional louvers because of the requirement that the louver be full closed at -95 C & fully open at 0 C . To achieve these goals

a trade study was performed to arrive at an initial concept that would utilize a bimetal actuator that has a much smaller change in length compared to traditional bimetals. Upon studying various potential bimetals, the bimetal material chosen was TM-5, an alloy, for Clipper (as opposed to a different alloy, TM-2, used for traditional louvers). The slow change of length of the bimetal for a much larger change in temperature would ensure that for a given original length - same due to configurational/volume constraints - of the bimetal spiral coil, the angular change of the coil would be still 90° without any mechanical stress experienced (zero-stress state) between the two extreme (fully open to fully closed) hard stop locations (0° to 90°). This would avoid overstressing the coils that could lead to any permanent plastic distortion once they reach their hard stops.

During this trade study of arriving at alternative designs several concepts were arrived at and studied to a small extent. Besides the low temperature louver, these were:

- 1) Wax or motor actuated driven MLI blanket flap to open or close the radiator's view to space based on cold/hot conditions
- 2) A heat switch array between the HRS tubing and the radiator to vary the thermal coupling between the HRS fluid and the radiator depending on cold or hot conditions
- 3) Utilizing the traditional state of the art louver bimetal coils and allowing them to reach stressed states once they hit the hard stops
- 4) Dual (stacked on top of each other) traditional louvers on the radiator to minimize their heat loss in cold conditions while not significantly decreasing their heat loss capability in hot conditions
- 5) No louvers on the radiator

Design	Total Mass	Power	Switching ratio*	Calibration uncertainty	Reliability	Fault tolerance
Low flexivity louvers (Baseline)	20 kg	10 W	27	±15 °C	Risky due to small forces	Good
Wax actuator driven MLI flap	<20 kg	5-10 W	35	±3 °C (?)	Radiation concern, hysteresis, instability	Poor
Motor actuator driven MLI flap	< 20 kg	5-10 W	35	±2 °C (PRT)	Radiation, cold temperature	Poor
Wax actuated louver blades	20-23 kg	10 W	27	±3 °C (?)	Radiation	Good
Heat Switch array b/w HRS tubes and radiator (50 switches)	10 kg	17 W	21	±3 °C (?)	Good (they typically fall open)	+5 W if 1 switch failed closed
Heritage louver at -30 °C	20 kg	33 W	11	±3 °C	Good	Good
No louver at all ($A_{rad}=0.9 \text{ m}^2$)	6 kg	50 W	7	-	Amazing	Excellent
Two louvers in series	>35 kg	21.5 W	16	±15 °C	Risky to mount a louver on top of a louver	Good

Design	Heritage	Fidelity of predictions	Implementation	Impact on S/C	Launch loads	Cost	Recommended for additional consideration
Low flexivity louvers (Baseline)	None	Large uncertainty	Set point calibration/ hysteresis due to low forces	None	Needs to be tested	\$5M	Yes
Wax actuator driven MLI flap	None	Good	Needs mechanisms/ thermally couple wax to fluid /clutch for fault tolerance	Will it fit in launch vehicle at RT with flaps open	Launch locks	Similar to louver	No
Motor actuator driven MLI flap	None	Good	Needs mechanism to actuate flap / clutch for fault tolerance	E-box in vault + avionics	Launch locks	More than louvers	No
Wax actuated louver blades	None	Good	New mechanism for opening blades	None	Similar to standard louver	More than standard louvers	No
Heat Switch array b/w HRS tubes and radiator (50 switches)	To be determined	Support structure to be accounted for	Straight forward	None	Needs stress analysis	Similar to louver	Yes
Heritage louver heated to -30 °C	lots	Good	easy	none	Need to assess for SLS	\$5M	Yes (if heated to -30 C)
No louver at all ($A_{rad}=0.9 \text{ m}^2$)	lots	Good	easy	none	none	cheap	No
Two louvers in series	none	Some uncertainty	Mechanical consideration	none	Need to assess	\$10 M	No

Table 2. Tradeoff of Various Design Concepts Investigated

The trade study yielded the conclusion that the use of a low temperature louver was the optimal balance between several system level resources and parameters. The affected parameters studied were: total mass, power, switching ratios, calibration uncertainty, reliability, fault tolerance, heritage, fidelity of performance predictions, implementation impact, and impact on spacecraft & its configuration, launch loads and costs.

The angular change per unit temperature change is known as the flexivity of the bimetal spiral coils. A byproduct of employing these low flexivity bimetals is that they also generate very small forces & torques. Any stiction due to friction between the louver blade bearings, gravity effects during ground testing & CTE effects could lead to these temperature induced forces (produced by the bimetal spiral spring) being overpowered. This could lead to hysteresis or jamming concerns and difficulty in achieving desired set points, which could lead to reduction of robustness. To alleviate these concerns, a development louver unit utilizing the low flexivity bimetal coil was assembled and is undergoing testing. Initial testing validated this design concept by exhibiting a 60 C control range with fully closed blades at >-95 C and fully open at -5 C.

Since there are eight louver assemblies utilized for the radiator, and each louver has several blade pairs, the overall louver system is very tolerant to failure of any blade.

VI. Conclusions

Several new technologies have been developed for the Europa Clipper mission and are being implemented in the Clipper spacecraft. All these are mission enablers, with the primary focus being power conservation due to severe limitations on available power at extreme distances from the Sun (5.6 A.U.). The ones described in this paper consist of dual MLI blankets, two passive thermal control valves in series and low temperature louvers. Development tests have been conducted on all of these and those tests have validated their basic designs. Additional testing is planned to further validate them in engineering models followed by test of their flight versions. All these technologies will provide either direct or modified versions for use in a wide variety of flight projects.

Acknowledgments

The work described in this paper was carried out at the Jet Propulsion Laboratory, California Institute of Technology, under a contract with the National Aeronautics and Space Administration. Copyright 2019 California Institute of Technology. Government sponsorship acknowledged.

References

- ¹Bhandari, P., Birur, G.C., and Gram, M.B., "Mechanical Pumped Cooling Loop for Spacecraft Thermal Control," SAE Technical Paper No. 961488, 26th International Conference on Environmental Systems, Monterey, California, July 8-11, 1996.
- ²Birur, G.C., Bhandari, P., Gram, M.B., and Durkee, J., "Integrated Pump Assembly- An Active Cooling System for Mars Pathfinder Thermal Control," SAE Technical Paper No. 961489, 26th International Conference on Environmental Systems, Monterey, California, July 8-11, 1996.
- ³Birur, G. and P. Bhandari, "Mars Pathfinder Active Thermal Control System: Ground and Flight Performance of a Mechanically Pumped Loop," Paper No AIAA-97-2469, 32nd Thermophysics Conference, Atlanta, GA, June 23-25, 1997.
- ⁴Birur, G.C. and Bhandari, P., "Mars Pathfinder Active Heat Rejection System: Successful Flight Demonstration of a Mechanically Pumped Cooling Loop," SAE Technical Paper No. 981684, 28th international Conference on Environmental Systems, Danvers, Massachusetts, July 13-16, 1998.
- ⁵Lam, L., Birur, G., and Bhandari, P., "Pumped Fluid Loops," *Satellite Thermal Control Handbook (2nd edition)*, Ed. D. Gilmore, Aerospace Corporation, El Segundo, California, 2002.
- ⁶Ganapathi, G., Birur, G., Tsuyuki, G., and Krylo, R., "Active Heat Rejection System on Mars Exploration Rover – Design Changes from Mars Pathfinder", Space Technology Applications International Forum 2003, Albuquerque, NM, February 2003.
- ⁷Tsuyuki, G., Ganapathi, G., Bame, D., Patzold, J., Fisher, R., and Theriault, L., "The Hardware Challenges for the Mars Exploration Rover Heat Rejection System," AIP Conference Proceedings, Vol. 699(1), pp. 59-70. February 2004.
- ⁸Bhandari, P., Birur, G., et al., "Mars Science Laboratory Thermal Control Architecture," SAE 2005-01-2828, 35th International Conference on Environmental Systems, Rome, Italy, July 2005.
- ⁹Bhandari, P., et al, "Mars Science Laboratory Rover Thermal Control Using a Mechanically Pumped Fluid Loop", Space Technology & Applications International Forum (STAIF-2006), March, 2006
- ¹⁰Birur, G., Bhandari, P., Prina, M., Bame, D., Yavrouian, A., and Plett, G., "Mechanically Pumped Fluid Loop Technologies for Thermal Control of Future Mars Rovers," SAE 2006-01-2035, 36th International Conference on Environmental Systems, Norfolk, Virginia, July 2006.

¹¹Birur, G.C., Prina, M, Bhandari, P, et al, "Development of Passively Actuated Thermal Control Valves for Passive Thermal Control of Mechanically Pumped Single Phase Fluid Loops for Space Applications." SAE 2008-01-2002 , 38th International Conference on Environmental Systems, San Francisco, California, June 29-July 2, 2008.

¹²Bhandari, P., Birur, G.C., et al, "Mechanically Pumped Fluid Loop Heat Rejection & Recovery Systems For Thermal Control on Martian Surface – Case Study of The Mars Science Laboratory," Panel Discussion: Mars and Beyond, 36th International Conference on Environmental Systems, Norfolk, Virginia, July 2006.

¹³Paris, A.D. et al, "Thermal Design of the Mars Science Laboratory Powered Descent Vehicle," SAE 2008-01-2001 38th International Conference on Environmental Systems, San Francisco, California, June 29-July 2, 2008

¹⁴Bhandari, P., Birur, G., et al. "Mars Science Laboratory Mechanically Pumped Fluid Loop for Thermal Control – Design, Implementation, and Testing", SAE 2009-01-2437, 39th International Conference on Environmental Systems, Savannah, Georgia, July 2009

¹⁵Mastropietro, A.J., et al., "Design and Preliminary Thermal Performance of the Mars Science Laboratory Rover Heat Exchangers," AIAA-2010-6194, 40th International Conference on Environmental Systems, Barcelona, Spain, July 11-15, 2010

¹⁶Paris, A.D., Novak, K.N., et al., "Overview of the Mars Science Laboratory Cruise Phase System Thermal Vacuum Test," AIAA-2010-6189, 40th International Conference on Environmental Systems, Barcelona, Spain, July 11-15, 2010

¹⁷Novak, K.S, Kempenaar, J.E., Liu, Y., Bhandari, P., and Dudik, B.A., "Mars Science Laboratory System Thermal Test," AIAA-2012-xxxx, 42nd International Conference on Environmental Systems, San Diego, California, July 15-19, 2012.

¹⁸Bhandari, P., Birur, G., et al. "Mars Science Laboratory Rover Launch Pad Thermal Control," AIAA-2011-5116, Portland, Oregon, July 2011

¹⁹Mastropietro, A.J., et al., "Launch Pad Closeout Operations for the Mars Science Laboratory's Heat Rejection System," AIAA-2012-xxxx, 42nd International Conference on Environmental Systems, San Diego, California, July 15-19, 2012

²⁰Bhandari, P., Birur, G.C., et al, "Design of Accumulators and Liquid/Gas Charging of Single Phase Mechanically Pumped Fluid Loop Heat Rejection Systems" AIAA-2012-xxxx, 42nd International Conference on Environmental Systems, San Diego, California, July 2012.

²¹Paris, A.D., Kelly, F.P., Kempenaar, J.E., and Novak, K., "In-Flight Performance of the Mars Science Laboratory Spacecraft Cruise Phase Thermal Control Systems," AIAA-2012-xxxx, 42nd International Conference on Environmental Systems, San Diego, California, July 15-19, 2012

²²Birur, G.C., et al. "Development of Passively Actuated Thermal Control Valves for Passive Control of Mechanically Pumped Single-Phase Fluid Loops for Space Applications" *ICES-2008-01-2002*, 38th International Conference on Environmental Systems, June 29-July 2 2008, San Francisco, CA, USA.

²³Birur, G.C., et al. "From Concept to Flight: An Active Fluid Loop Based Thermal Control System for Mars Science Laboratory Rover" *ICES-2012*, 42th International Conference on Environmental Systems, July 15-19, 2012, San Diego, CA, USA.

²⁴Lin, E.I., and Kwok, Stultz, J.W., and Reeve, R.T., "Test Derived Effective Emittance for Cassini MLI Blankets and Heat Loss Characteristics in the Vicinity of Seams," *Journal of Thermophysics and Heat Transfer*, Vol 10. No. 2, April-June 1996.

²⁵Miyakita, T., et al, "Evaluation of Thermal Insulation Performance of a New Multi-Layer Insulation with Non-Interlayer-Contact Spacers," *ICES-2015-220*, 45th International Conference on Environmental Systems, 12-16 July 2015, Bellevue, WA, USA.

²⁶Mills, G., "Modeling and Testing of Integrated and Load Responsive Multilayer Insulation," *Spacecraft Thermal Control Workshop*, Aerospace Corporation, March 20, 2012, Los Angeles, CA, USA.

²⁷Smith, C., et al. "Performance of multi-layer insulation for spacecraft instruments at cryogenic temperatures," 46th International Conference on Environmental Systems, 10-14 July 2016, Vienna, Austria.

²⁸Bhandari, P., et al. "A Dual Multilayer Insulation Blanket Concept to Radically Reduce Heat Loss From Thermally Controlled Spacecraft and Instruments," *ICES-2018-24*, 48th International Conference on Environmental Systems, 8-12 July 2018, Albuquerque, NM, USA.

²⁹Keller, C.W., et al. "Final Report: Thermal Performance of Multilayer Insulation," April 5 1974, Lockheed Missile & Space Systems, Sunnyvale, CA, USA.

³⁰Bhandari, P., et al. "Mars Science Laboratory Mechanically Pumped Fluid Loop for Thermal Control – Design, Implementation, and Testing," *ICES-2009-24*, 39th International Conference on Environmental Systems, 12-16 July 2009, Savannah, GA, USA.

³¹Gilmore, D, "Spacecraft Thermal Control Handbook," Chapter 9, Louvers, Aerospace Press, AIAA.